THE EFFECT OF SUPPRESSION OF THE SUPERCONDUCTING GAP FUNCTION AT NORMAL METAL - d-WAVE SUPERCONDUCTOR INTERFACE ON THE TUNNELING SPECTRUM

Miss Sukanya Nilmoung

A Thesis Submitted in Partial Fulfillment of the Requirements

for the Degree of Master of Science in Physics

Suranaree University of Technology

Academic Year 2003

ISBN 974-533-288-7

THE EFFECT OF SUPPRESSION OF THE SUPERCONDUCTING GAP FUNCTION AT NORMAL METAL - *d*-WAVE SUPERCONDUCTOR INTERFACE ON THE TUNNELING SPECTRUM

Suranaree University of Technology has approved this thesis submitted in partial fulfillment of the requirements for a Master's Degree

Thesis Examining Committee

(Asst. Prof. Dr. Prapan Manyum)
Chairperson

(Dr. Puangratana Pairor)
Member (Thesis Advisor)

(Dr. Sukit Limpijumnong)
Member

(Assoc. Prof. Dr. Prasart Suebka)
Member

(Dr. Saroj Rujirawat)
Member

(Assoc. Prof. Dr. Sarawut Sujitjorn)
Vice Rector for Academic Affairs

(Assoc. Prof. Dr. Prasart Suebka)
Dean of the Institute of Science

สุกัญญา นิลม่วง : ผลของการลดลงของฟังก์ชันช่องว่างพลังงานของตัวนำยวดยิ่งที่รอยต่อของโลหะปกติ – ตัวนำยวดยิ่งแบบ-ดี-เวฟต่อสเปกตรัมการทะลุผ่าน (THE EFFECT OF SUPPRESSION OF THE SUPERCONDUCTING GAP FUNCTION AT NORMAL METAL - *d*-WAVE SUPERCONDUCTOR INTERFACE ON THE TUNNELING SPECTRUM) อาจารย์ที่ปรึกษา: ดร. พวงรัตน์ ไพเราะ, 39 หน้า.

ISBN 974-533-288-7

วิทยานิพนธ์นี้เป็นการศึกษาเชิงทฤษฎีเกี่ยวกับผลของการลดลงของช่องว่างพลังงานต่อสเปกตรัมการทะลุผ่านรอยต่อระนาบ{110}ของโลหะปกติ-ตัวนำยวดยิ่งแบบ-ดี-เวฟ ค่ากระแสและค่าความนำไฟฟ้าทะลุผ่านหาได้จากวิธีการกระเจิงที่เรียกว่า รูปนัยนิยม ของ Blonder-Tinkham-Klapwijk (BTK) ผลลัพธ์ทั้งหมดที่ได้อยู่ในช่วงค่าพลังงานของอนุภาคซึ่งน้อยกว่าช่องว่างพลังงานสูงสุดมาก ๆ และที่อุณหภูมิศูนย์เคลวิน พบว่าสำหรับผิวรอยต่อ{110} ยอดสูงสุดที่ความต่างศักย์เป็นศูนย์ของเส้นสเปกตรัมค่าความนำการทะลุผ่านไม่ปรากฏขึ้นเลย ถ้าขนาดของช่องว่างพลังงานของตัวนำยวดยิ่งลดลงจนเป็นศูนย์ที่รอยต่อ ผลที่ได้นี้อาจนำไปใช้อธิบายการหายไปของยอดสูงสุดที่ความต่างศักย์เป็นศูนย์ในการทดลองการทะลุผ่านหลายการทดลองที่เกี่ยวกับการทะลุผ่านรอยต่อในระนาบเอบีของตัวนำยวดยิ่งอุณหภูมิสูงหลายตัวได้ ยอดสูงสุดที่ความต่างศักย์เป็นศูนย์สามารถเกิดขึ้นได้ ถ้าขนาดของช่องว่างพลังงานของตัวนำยวดยิ่งลดลงไม่เป็นศูนย์อย่างสมบูรณ์ที่รอยต่อ ความกว้างของยอดสูงสุดที่ความต่างศักย์เป็นศูนย์ขึ้นอย่างมากกับระดับการลดลงของช่องว่างพลังงานที่รอยต่อ การลดลงของช่องว่างพลังงานที่รอยต่อเพิ่มขึ้นมากเท่าใด ยอดสูงสุดที่ความต่างศักย์เป็นศูนย์ก็จะแคบลง ความสูงของยอดสูงสุดที่ความต่างศักย์เป็นศูนย์ขึ้นกับความโปร่งของรอยต่อ

สาขาวิชาฟิสิกส์ ลายมือชื่อนักศึกษา สุกัญญา นิลม่วง

ปีการศึกษา 2546 ลายมือชื่ออาจารย์ที่ปรึกษา พวงรัตน์ ไพเราะ

ลายมือชื่ออาจารย์ที่ปรึกษาร่วม

SUKANYA NILMOUNG : THE EFFECT OF SUPPRESSION OF THE SUPERCONDUCTING GAP FUNCTION AT NORMAL METAL - *d*-WAVE SUPERCONDUCTOR INTERFACE ON THE TUNNELING SPECTRUM

THESIS ADVISOR: PUANGRATANA PAIROR, Ph.D. 39 PP.

ISBN 974-533-288-7

N-S JUNCTION/ *d*-WAVE SUPERCONDUCTOR / TUNNELING CONDUCTANCE SPECTRUM/ ZERO BIAS CONDUCTANCE PEAK

This thesis is the theoretical study of the effect of the gap suppression on tunneling spectroscopy of normal metal - $d_{x^2-y^2}$-wave superconductor $\{110\}$ junctions. The current and the tunneling conductance are obtained by the scattering method, known as the Blonder-Tinkham-Klapwijk (BTK) formalism. All of the results are obtained over the quasiparticle energy range that is much smaller than the gap maximum and at zero temperature. It is found that at $\{110\}$ surfaces Zero Bias Conductance Peak (ZBCP) in tunneling conductance spectra can be absent if the value of the superconducting gap at the interface is suppressed to zero. This result may be used to explain the absence of the ZBCP in many tunneling experiments done on the *ab*-plane tunneling junctions of many high temperature cuprate superconductors. The ZBCP can be present if the value of superconducting gap at the interface is not completely suppressed. The width of ZBCP strongly depends on the degree of the gap suppression at interface. The more suppressed the gap is, the narrower the ZBCP. The height of ZBCP depends on the transparency of the junction.

School of Physics
Academic Year 2003

Student's Signature Sukanya Nilmoung
Advisor's Signature
Co-advisor's Signature

Acknowledgements

All through this thesis work, I have got a lot of help from many people. First of all, I would like to express my sincere gratitude to my thesis advisor Dr. Puangratana Pairor, for her long term guidance on all problems throughout this work.

I am also grateful to all the lecturers of the School of Physics, Institute of Science, Suranaree University of Technology: Prof. Dr. Eduard B Manokian, Assoc. Prof. Dr. Prasart Suebka, Assoc. Prof. Dr. Samnao Phatisena, Asst. Prof. Dr. Yupeng Yan, Dr. Chinorat Kobdaj, Dr. Saroj Rujirawat, Dr. Sukit Limpijumnong, Dr. Supagorn Rugmai, Dr. Worasit Uchai, who have taught me in all graduate courses.

I would also like to especially thank Assoc. Prof. Dr. Prasart Suebka, Dr. Prapan Manyum, Dr. Saroj Rujirawat and Dr. Sukit Limpijumnong for being on my thesis committee.

I would like to thank Mr. Jessada Tanthanuch, Mr. Sampart Cheedket and all physics graduate students at Suranaree University of Technology for their friendly support and guidance.

Finally, I would like to thank my parents for their never-ending support and encouragement over all the years of my life.

Sukanya Nilmoung

Contents

Contents (continued)

List of Figures

List of figures (continued)

Figure **Page**

Chapter I

Introduction

1.1 Motivation

High temperature superconductivity was first discovered in ceramic $(LaBa)_3CuO_4$ with the transition temperature (T_c) approximately 30 K by Bednorz and Muller in 1986 (Bednorz, J. G., Müller, K. A. 1986), and right after this discovery many other CuO_2 based materials, such as $YBa_2Cu_3O_7$ (Wu, M. K., *et al.*, 1987) and $Bi_2Sr_2Ca_2Cu_3O_{10}$ (Maeda, H., *et al.*, 1988) with their T_c's higher than liquid nitrogen (77 K) were also discovered. These cuprate superconductors do not behave like ordinary Bardeen-Cooper-Schrieffer (BCS) superconductors. For instance, their T_c's are unusually high, their coherence lengths are extremely short (Burns, G. 1992; Parks, R. D. 1996; Tinkham, M. 1996) and their isotope effects are smaller than those of conventional superconductors (Bourne, L. C., *et al.*, 1987; Batlogg, B., *et al.*, 1987; Pascal J. Y., *et al.*, 1988; Mascarenhas, A., *et al.*, 1998). Also, the superconducting gaps of these materials are much larger than those of BCS superconductors, i.e., $2\Delta/k_BT_c > 3.54$ (Wei, J. Y. T., *et al.*, 1998). As it turns out, the symmetry of the superconducting order parameter of these materials is not s-wave, like that of the conventional superconductors. The phase-sensitive Superconducting QUuantum Interference Devices (SQUID) experiment (Wollman, D. A., *et al.*, 1993; Brawner, D.A., and Ott, H. R. 1994) and the tricrystal magnetometry (Tsuei, C. C., *et al.*, 1994; Kirtley, J. R., *et al.*, 1996) indicate that their gap symmetry is $d_{x^2-y^2}$-wave, i.e., it has nodes along the $\pm 45°$ and $\pm 135°$ directions in the momentum space. Many tunneling experiments also show the linear dependence of the conductance curve at low voltages and a zero bias conductance peak (ZBCP) (Alff, L., *et al.*, 1997; Covington, M., *et al.*, 1997; Wei, J. Y. T. *et al.*, 1998; Sinha, S., and Ng, K.-W. 1998). These tunneling characteristics are also consistent with the $d_{x^2-y^2}$-wave symmetry of the energy gap. That is, the presence of the low energy excitations, which result in a linear dependence of the density of states at low energies, are due to the existence of the nodes. A ZBCP in the tunnelling conductance spectrum implies that there exist a number of bound states at zero energy (relative to the Fermi level). These zero energy bound states are linear combinations of two quasiparticle excitations with the gaps of opposite signs, a consequence of the $d_{x^2-y^2}$ gap symmetry.

The mechanism that causes superconductivity in high-temperature superconductors materials is still a mystery. There have been a lot of theoretical and experimental work constantly done on these materials to gain more understanding about their nature. This master thesis is one of the theoretical ones. In particular, this thesis is the study of tunnelling spectroscopy of a normal metal - $d_{x^2-y^2}$-wave superconductor junction.

The tunneling spectroscopy has been used to study the quasiparticle density of states (DOS) in superconductors since 1960 (Giaever, I. 1960). It provides a direct measurement of the superconducting gap (Duke, C. B. 1969; Wolf, E. L. 1985). In the experiment, the tunneling conductance is measured as the applied voltage is changed. The tunneling conductance, in the tunneling limit, is proportional to the local density of states of superconductor (Tanaka, Y., and Kashiwaya, S. 1995). In case of normal metal - isotropic s-wave superconductors interfaces, the tunneling conductance spectra are independent of the crystal orientation, because the local density of states is the same as the bulk density of states. On the contrary, the tunneling conductance spectra of normal metal - anisotropic superconductors depend strongly on the crystal orientation of the superconductor. In particular, for $d_{x^2-y^2}$-wave superconductors junctions with $\{100\}$ surfaces, the curve of conductance *vs* applied voltage is linear at low voltages and peaks at the maximum of the energy gap. No ZBCP is found for these surfaces. For the junctions with surface orientations away from {100}, the conductance spectra contain ZBCPs, indicating as mentioned earlier the formation of quasiparticle surface bound states at zero energy (Hu, C-R. 1994; Kashiwaya, S., *et al.*, 1996).

Theoretically, a ZBCP should not show up in the tunneling spectra of a normal metal - $d_{x^2-y^2}$-wave superconductor junction with {100} surface orientation, because the gap values of the two outgoing quasiparticles have the same sign. However, in many tunneling experiments (Covington, M., *et al.*, 1997; Wei, J. Y. T., *et al.*, 1998; Iguchi, I., *et al.*, 2000) the conductance spectra of these junctions contain ZBCPs. This unexpected show of ZBCP may be explained by the fact that the real junctions are not smooth. The roughness of the surface of the superconductor causes misorientations relative to the average interface normal and can lead to surface induced Andreev scattering, which reveals as a ZBCP in the conductance spectra even for {100} surface orientations (Fogelström, M., *et al.*, 1997; Lück, T., *et al.*, 2001). In addition, the absence of ZBCP in the conductance spectra of some *ab*-plane junctions with the orientations away from {100} is another unexpected experimental results found in some high temperature superconductors (Cucolo, A. M., *et al.*, 1994, Wei, J. Y. T., *et al.*, 1998). Also, the height of ZBCP in the tunneling conductance spectra of the {110} junctions in many tunneling experiments (Alff, L., *et al.*, 1998; Aubin, H., *et al.*, 2002) is not as high as it should be. The interpretation of this unexpected absence and small ZBCP in the spectra of {110} junction has not been clearly made.

In most theoretical studies of the normal metal - $d_{x^2-y^2}$-wave superconductor tunneling spectroscopy, it is assumed for simplicity that the gap function is zero on the normal side and is finite and independent of the distance measured from the interface on the superconducting side. That is, both proximity effect and the suppression of the gap function near the interface, which occurs over a coherence length, are ignored. This assumption is called the step function model, which is in fact is not quite true, but at the same time is not far-fetched for cuprates, whose coherence lengths are about

10-15 Å (Parks, R. D. 1996; Tinkham, M. 1996). Therefore, it is interesting to study how the suppression of the gap near the normal metal and $d_{x^2-y^2}$-wave superconductor interface may affect the feature, like ZBCP, in the tunneling conductance spectra of $d_{x^2-y^2}$-wave superconductors.

This thesis contains the theoretical study of tunneling spectroscopy of $d_{x^2-y^2}$-wave superconductors. In particular, it focuses on the study of the effect of the gap suppression near the interface on the tunneling spectroscopy of normal metal - $d_{x^2-y^2}$-wave superconductor junctions. This work may be able to help to clarify the interpretation about the unexpected absence of ZBCP in the tunneling conductance spectra of $\{110\}$ junctions.

1.2 Methods and Assumptions

The method used to study the tunneling spectroscopy in this thesis is the so-called Blonder-Tinkham-Klapwijk (BTK) formalism (Blonder, G. E., *et al.*, 1982). This formalism is basically a scattering method, which is used to find the reflection and transmission probabilities of a junction. The basic idea of this method is as follows. An incident electron comes from the normal side and is reflected and transmitted at the interface. At the boundary of the normal metal and superconductor, there occur two reflections and two transmissions processes (see Fig. 1.1). The two reflections processes are the normal reflection, which reduces the number of electrons crossing the boundary, and the Andreev reflection, which does the opposite (enhancing the number of electrons across the junction) (Andreev, A. F. 1964). The two transmission processes involve the transmission through the interface with a wave vector on the same side of the Fermi surface and the transmission with a wave vector crossing through the Fermi surface. The wave function of the normal metal can therefore be written as the combination of the incoming electron and the two reflections, and the wave function of the superconductor can be written as the combination of the two transmitted excitations. With appropriate matching conditions at the interface, all the reflection and transmission probabilities can be obtained. The current and tunneling conductance of the junction can then be calculated from these reflection and transmission probabilities.

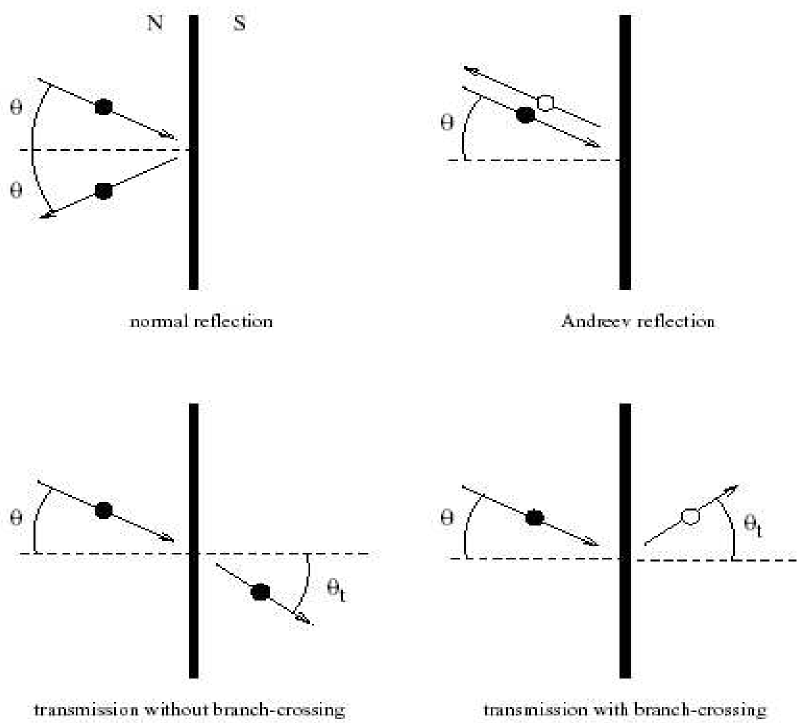

Figure 1.1: Schematic diagram of the directions of reflections and transmissions at normal metal - superconductor interface (Mortensen, N. A. 1998)

In this thesis, the effect of the gap suppression near the surface on ZBCP of a normal metal - $d_{x^2-y^2}$-wave superconductor junction with $\{110\}$ orientations is investigated. Because the $d_{x^2-y^2}$-wave superconductors of interest are quasi-two dimensional, the Fermi surfaces of the superconductors are assumed to be cylindrical and so are those of normal metals. The real Fermi surface affect other features in the conductance spectrum but does not affect the ZBCP (Pairor, P., and Walker, M. B. 2002). The proximity effect is ignored in this study and all the calculations are done at the energy much less than the maximum gap and at zero temperature.

1.3 Outline of Thesis

This thesis contains the theoretical study of the effect of suppression of the superconducting gap function at the interface of normal metal and $d_{x^2-y^2}$-wave superconductor. The organization of this thesis is as follows.

In the next chapter, the review of tunneling spectroscopy of normal metal - $d_{x^2-y^2}$-wave superconductor junction at zero temperatures in the step function model is reviewed. In this model, the gap function is taken to be zero in the normal metal, and finite and independent of position in the superconductor. The conductance spectra of the junctions with $\{110\}$ orientation are investigated using this model for later comparison.

In chapter III, a brief review of the properties of a $d_{x^2-y^2}$-wave superconductor near a surface is given. Also, a formulation to calculate the current and the tunneling conductance, which includes the effect of the suppression of superconducting gap, is presented. All the results are obtained at the energy much less than the gap maximum and at zero temperature. All the results of the calculations are also discussed in details in this chapter.

The conclusions of this thesis are addressed in chapter IV.

Chapter II

Normal metal - $d_{x^2-y^2}$-wave Superconductor Junctions with {110} Interfaces in the Step Function Model

2.1 Introduction

In this chapter, the ab-plane tunneling spectroscopy of a normal metal - $d_{x^2-y^2}$-wave superconductor junction with {110} surface orientation is investigated using the step function model. In particular, the feature that is mainly focussed in the tunneling spectrum is ZBCP. The factors, on which the width and height of ZBCP depend, will be studied.

The junction is modelled as an infinite system with the insulating interface plane being the xy plane at $x = 0$, as depicted in Fig. 2.1.

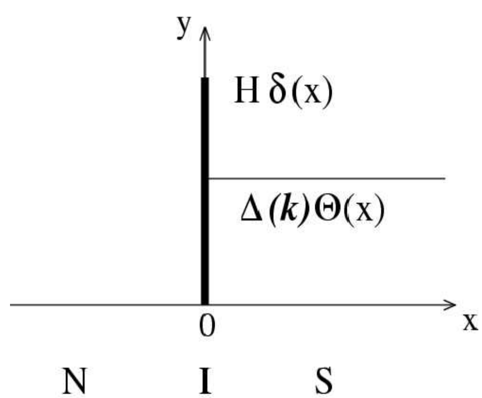

Figure 2.1: The sketch of the normal metal - $d_{x^2-y^2}$-wave superconductor junction in the step function model.

The $x > 0$ region is the superconductor, whereas the $x < 0$ region is the normal metal. The potential barrier located at the interface is described by a delta function,

$$U(\vec{r}) = H\delta(x), \tag{2.1}$$

where H represents the strength of barrier. In the step function model, the gap function is taken to be zero on the normal side and to be finite and independent of the position on the superconducting side, i.e.,

$$\Delta(\vec{k}) = \Delta_d(\vec{k})\Theta(x), \tag{2.2}$$

where $\Theta(x)$ is the Heaviside step function. $\triangle_d(\vec{k}) = \Delta_d(\theta) = \Delta_{max}\cos[2(\theta-\alpha)]$, where θ is the angle between the wave vector on the Fermi surface and the interface normal vector, and α is the angle between the a-axis of the superconductor and the

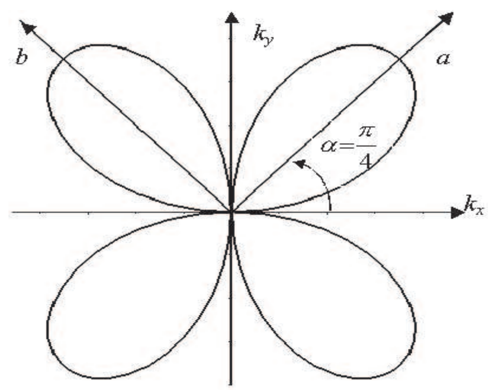

Figure 2.2: The sketch of $d_{x^2-y^2}$-wave superconductor gap function in the case where a-axis is tilted with an angle $\alpha = \pi/4$. (α is defined in the text.)

interface normal vector.

The orientation of interest is {110}, which corresponds to $\alpha = \pi/4$ (see Fig. 2.2), so the gap function of $d_{x^2-y^2}$-wave superconductor for this orientation is

$$\triangle_d(\theta) = \Delta_{max}\sin(2\theta). \tag{2.3}$$

In order to obtain the current and the tunneling conductance, the scattering probabilities at interface are calculated by using the scattering method known as the Blonder-Tinkham-Klapwijk (BTK) formalism (Blonder, G. E., *et al.*, 1982). This method makes use of the following Bogoluibov-de Gennes equations, which are two coupled Schrӧdinger equations:

$$\left(-\frac{\hbar^2}{2m}\nabla^2 + H\delta(x) - E_F\right)u(\overrightarrow{r}) + \triangle_d(\theta)\Theta(x)v(\overrightarrow{r}) = Eu(\overrightarrow{r}),$$

$$\triangle_d(\theta)\Theta(x)u(\overrightarrow{r}) + \left(\frac{\hbar^2}{2m}\nabla^2 - H\delta(x) - E_F\right)v(\overrightarrow{r}) = Ev(\overrightarrow{r}), \tag{2.4}$$

where E_F is the Fermi energy, m is the electron mass, the energy of the quasiparticle E is measured from the Fermi level, and $u(\vec{r})$, $v(\vec{r})$ are the electron-like and hole-like components of the wave function respectively. Since the system is translational invariant along the y direction, the momentum parallel to the interface, $k_y = k_F\sin\theta$, is conserved.

Assume an electron with the x-component of momentum, q^+, is incident on the interface from the normal side with energy E and it has the direction that makes an angle θ with the interface normal (see Fig. 2.3 (c)). For each energy E, there are four possible other states, i.e., the states with the x-component of the momentum equal to $q^-, -q^+, k^+$ and $-k^-$ respectively, as shown in Fig. 2.3. The states with q^- and $-q^+$ are Andreev reflected hole and normal reflected electron respectively. The states with k^+ and $-k^-$ are electron-like and hole-like transmitted excitations respectively. So, the wave function of normal metal side is the combination of the wave functions of the incident electron, the Andreev reflected hole and normal reflected electron. The normal metal wave function thus is written as

$$\Psi_N(x<0,y) = \left(\begin{bmatrix} 1 \\ 0 \end{bmatrix} e^{iq^+x} + a\begin{bmatrix} 0 \\ 1 \end{bmatrix} e^{iq^-x} + b\begin{bmatrix} 1 \\ 0 \end{bmatrix} e^{-iq^+x}\right) e^{ik_y y}. \tag{2.5}$$

where a and b are the amplitudes of Andreev and normal reflections, respectively.

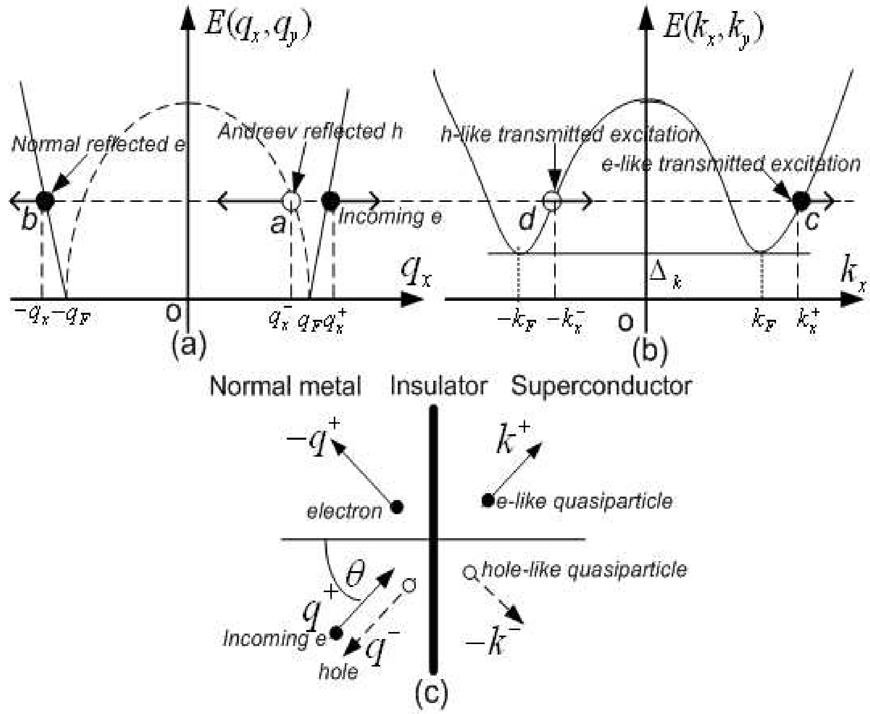

Figure 2.3: Schematic diagrams of (a) excitation energy E vs the x-component, q_x, of the wave vector of the normal metal and (b) the quasiparticle energies with the x-component, k_x, of the wave vector of the superconductor. The full dots ($\bullet$) represent electron-like quasiparticles and open dots ($\circ$) represent hole-like quasiparticles. The associated arrows in (a), (b) and (c) point in the direction of group velocity and a, b, c, and d are the amplitudes representing the Andreev reflection, the normal reflection, the same branch transmission and the cross-branch transmission respectively.

The wave function of the superconductor side is the combination of the two transmitted excitations. That is,

$$\Psi_S(x>0,y) = \left(c \begin{bmatrix} u_{k^+} \\ v_{k^+} \end{bmatrix} e^{ik^+x} + d \begin{bmatrix} u_{-k^-} \\ v_{-k^-} \end{bmatrix} e^{-ik^-x} \right) e^{ik_y y}. \tag{2.6}$$

where c and d are the amplitudes of two transmissions. u_k and v_k are the electron-like and hole-like quasiparticle excitation amplitudes and are defined as

$$u_k = \frac{E+\xi_k}{\sqrt{|E+\xi_k|^2 + |\,\Delta_d(\theta)|^2}}, \tag{2.7}$$

$$v_k = \frac{\Delta_d(\theta)}{\sqrt{|E+\xi_k|^2 + |\,\Delta_d(\theta)|^2}}, \tag{2.8}$$

so that $|u_k|^2 + |v_k|^2 = 1$. E is the quasiparticle energy in the bulk of superconductor and ξ_k is the one-electron energy of the state k relative to the fermi level in the normal state. The relation between E, ξ_k and $\Delta_d(\theta)$ is

$$E^2 = \xi_k^2 + \Delta_d^2(\theta), \tag{2.9}$$

In the case where $\alpha = \pi/4$, $\Delta_{-k^+} = -\Delta_{k^+}$ for all wave vector k. Also, $\xi_{-k} = \xi_k$ and $\xi_{k^\pm} = \pm\xi_k$. Thus, define

$$u_{k^+} \equiv u_k, \qquad v_{k^+} \equiv v_k, \tag{2.10}$$

and as a consequence,

$$u_{-k^-} = v_k, \qquad v_{-k^-} = -u_k, \tag{2.11}$$

Then the wave function of the superconductor becomes

$$\Psi_S(x>0,y) = \left(c \begin{bmatrix} u_k \\ v_k \end{bmatrix} e^{ik^+x} + d \begin{bmatrix} v_k \\ -u_k \end{bmatrix} e^{-ik^-x} \right) e^{ik_y y}. \tag{2.12}$$

Since the energy range of interest is of order meV, which is the order of energy gap and is usually much smaller than the Fermi energy, so approximately $q^+ = q^- = q_x$ and $k^+ = k^- = k_x$, where $q_x = q_F \cos\theta$ and $k_x = k_F \cos\theta$, respectively. The amplitudes a, b, c and d are found by using the matching condition of the two wave functions and the slopes of the wave functions at the interface. These matching conditions are as follows:

(i) Continuity of wave function at interface

$$\Psi_S(x=0) = \Psi_N(x=0) \equiv \Psi(0), \tag{2.13}$$

(ii) The discontinuity of the slopes of the junction at the interface

$$\left.\frac{\partial \Psi_S}{\partial x}\right|_{x=0^+} - \left.\frac{\partial \Psi_N}{\partial x}\right|_{x=0^-} = 2Z\,k_F\,\Psi(0), \tag{2.14}$$

where $Z = \frac{mH}{\hbar^2 k_F}$ is the unitless parameter that characterizes the barrier strength of the junction.

For simplicity, the magnitudes of the Fermi wave vectors of both normal metal and superconductor are taken to be the same, i.e., $q_F = k_F$. The unequal Fermi wave vectors leads to the same consequence as the increase in Z. Therefore, the amplitudes of two reflections and two transmissions are

$$\begin{aligned} a(E,\theta) &= \frac{-4u_k v_k \cos^2\theta}{-u_k^2(4\cos^2\theta + 4Z^2) - 4Z^2 v_k^2}, \\ b(E,\theta) &= \frac{(u_k^2+v_k^2)(-4iZcos\theta - 4Z^2)}{-u_k^2(4\cos^2\theta + 4Z^2) - 4Z^2 v_k^2}, \\ c(E,\theta) &= \frac{-2u_k\cos\theta(2\cos\theta - 2iZ)}{-u_k^2(4\cos^2\theta + 4Z^2) - 4Z^2 v_k^2}, \\ d(E,\theta) &= \frac{-4iZv_k\cos\theta}{-u_k^2(4\cos^2\theta + 4Z^2) - 4Z^2 v_k^2}. \end{aligned} \tag{2.15}$$

The magnitude of the current density of electron defined as

$$|J| = |\Psi^\dagger \Psi v_k|, \tag{2.16}$$

where $v_k = \frac{1}{\hbar}\frac{dE}{dk_x}$ is the group velocity in the x direction and $\Psi^\dagger$ is the adjoint of the wave function Ψ. The Andreev and normal reflection probabilities are defined as

$$\begin{aligned} A(E,\theta) &= \left|\frac{J_{Refl(a)}}{J_{Inc}}\right| = |a(E,\theta)|^2\left|\frac{q^-}{q^+}\right| = |a(E,\theta)|^2, \\ B(E,\theta) &= \left|\frac{J_{Refl(b)}}{J_{Inc}}\right| = |b(E,\theta)|^2\left|\frac{-q^+}{q^+}\right| = |b(E,\theta)|^2. \end{aligned} \tag{2.17}$$

The two transmission probabilities are equal to

$$\begin{aligned} C(E,\theta) &= \left|\frac{J_{Tran(c)}}{J_{Inc}}\right| = |c(E,\theta)|^2(|u_k|^2 - |v_k|^2)\left|\frac{k^+}{q^+}\right| = |c(E,\theta)|^2(|u_k|^2 - |v_k|^2), \\ D(E,\theta) &= \left|\frac{J_{Tran(d)}}{J_{Inc}}\right| = |d(E,\theta)|^2(|u_k|^2 - |v_k|^2)\left|\frac{-k^-}{q^+}\right| = |d(E,\theta)|^2(|u_k|^2 - |v_k|^2). \end{aligned} \tag{2.18}$$

The conservation of probability current density requires

$$A(E,\theta) + B(E,\theta) + C(E,\theta) + D(E,\theta) = 1, \tag{2.19}$$

In the case where the quasiparticle energy is much less than the maximum gap ($E \ll \Delta_{max}$), $C(E,\theta) = D(E,\theta) = 0$ and therefore

$$A(E,\theta) + B(E,\theta) = 1, \tag{2.20}$$

Thus, for $E \ll \Delta_{max}$, the number of electrons tunneling across the junction per one incident electron in the tunneling limit is

$$1 + A(E,\theta) - B(E,\theta) = 2A(E,\theta) = \frac{2(\frac{P_k \Delta_d(\theta)}{2})^2}{E^2 + (\frac{P_k \Delta_d(\theta)}{2})^2}, \tag{2.21}$$

This yields a Lorentzian-shaped peak at zero energy with the width equal to $\frac{P_k \Delta_d(\theta)}{2}$, where P_k is the probability of tunneling across the junction

$$P_k = \frac{\cos^2(\theta)}{Z^2 + \cos^2(\theta)}. \tag{2.22}$$

Figure 2.4 (a) shows the plots of $1 + A(E) - B(E)$ at different incident angle θ. The peak of $1 + A(E) - B(E) = 2$ appears at zero energy for all value of θ. It is not surprising that at $E = 0$ the number of the electrons crossing the junction is 2, because at this energy the Andreev reflection process, in which $2e$ is transferred into the superconductor (forming a cooper pair) is the only possible process. For the same junction transparency, the width of $1 + A(E) - B(E)$ depends on the value of the gap at each incident angle, $\Delta_d(\theta)$. At the same incident angle, the width of $1 + A(E) - B(E)$ is proportional to P_k, which is inversely proportional to Z^2 (see Fig. 2.5)

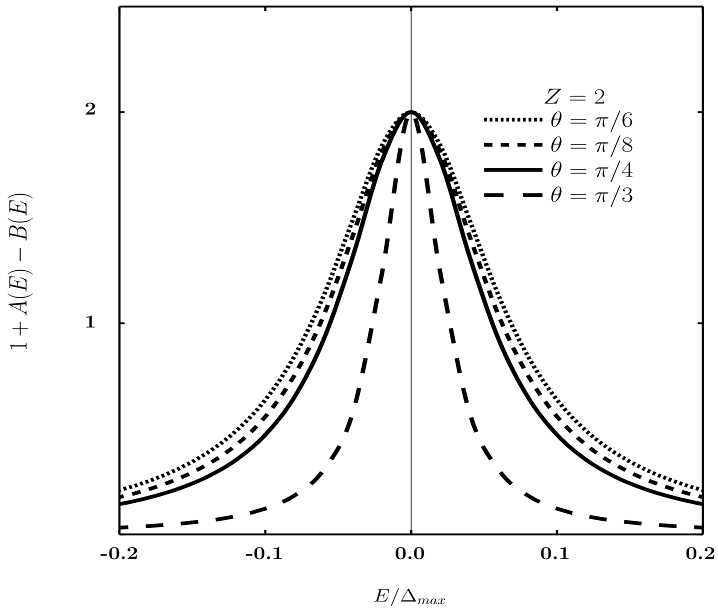

(a)

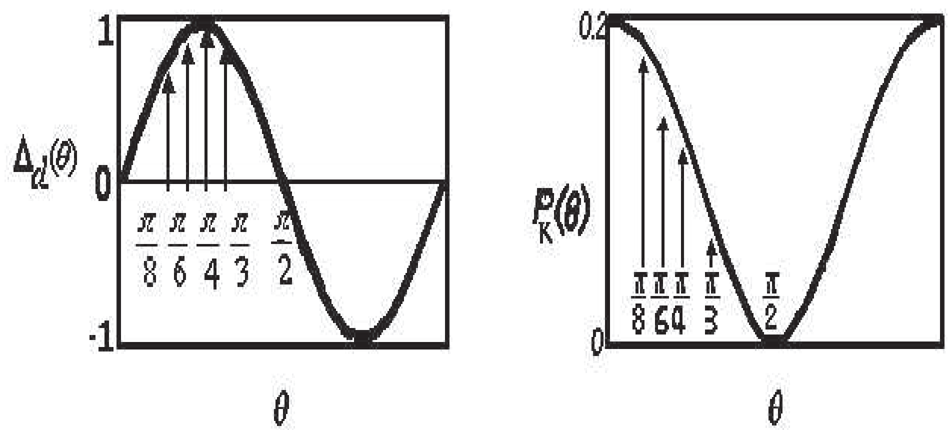

Figure 2.4: (a) The plots of $1 + A(E) - B(E)$ at different incident angles $\theta = \pi/3, \pi/4, \pi/6, \pi/8$ for $Z = 2$. (b) The angle θ dependence of $d_{x^2-y^2}$-wave superconducting gap. (c) The angle θ dependence of the probability of tunneling across the junction.

.

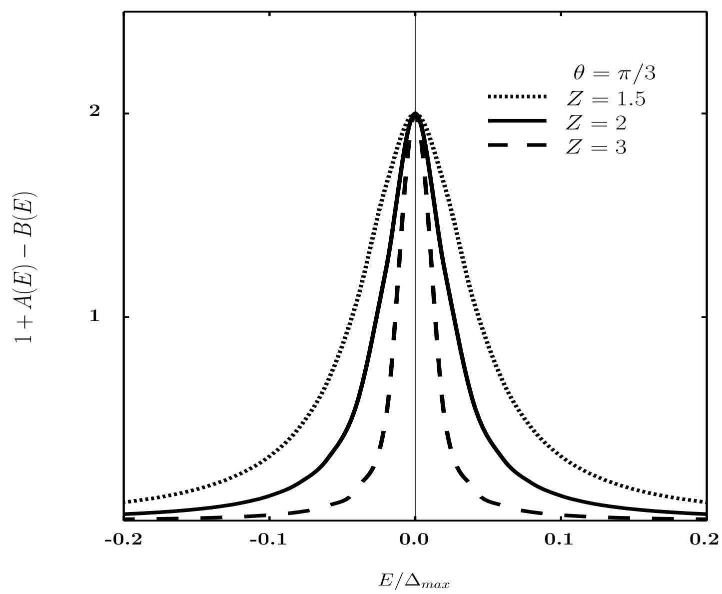

Figure 2.5: The plots of $1 + A(E) - B(E)$ for different $Z = 1.5, 2, 3$ at $\theta = \pi/3$.

2.2 The Tunneling Current and Tunneling Conductance

In a two dimensional system, the general relation for current density in the x-direction across the junction is given by

$$J = \sum_{k_x, k_y} n_k v_k e, \tag{2.23}$$

where v_k is the group velocities, e is the electron charge and n_k=$(1+A(E)-B(E)f(E)$, and $f(E)$ is the Fermi Dirac distribution function. The current flowing across junction from normal metal to $d_{x^2-y^2}$-wave superconductor with applied voltage V is therefore

$$I_{N \to S} = \frac{L^2 e}{4\pi^2 \hbar} \int_{-\infty}^{+\infty} \int_{-\infty}^{+\infty} dk_y dE (1 + A(E,\theta) - B(E,\theta)) f(E - eV). \tag{2.24}$$

and similarly the current flowing across junction from $d_{x^2-y^2}$-wave superconductor to normal metal is

$$I_{S \to N} = \frac{L^2 e}{4\pi^2 \hbar} \int_{-\infty}^{+\infty} \int_{-\infty}^{+\infty} dk_y dE (1 + A(E,\theta) - B(E,\theta)) f(E). \tag{2.25}$$

Thus, the net current crossing the junction is

$$\begin{aligned} I(eV,\theta) &= I_{N\to S} - I_{S\to N} \\ &= \frac{L^2 e}{4\pi^2\hbar}\int_{-\infty}^{+\infty}\int_{-\infty}^{+\infty} dk_y dE(1+A(E,\theta)-B(E,\theta))(f(E-eV)-f(E)), \end{aligned} \tag{2.26}$$

Since $k_y = k_F \sin\theta$ and then $dk_y = k_F \cos\theta d\theta$. So,

$$I_{NS}(eV,\theta) = \frac{L^2 e k_F}{4\pi^2\hbar}\int_{-\pi/2}^{+\pi/2} d\theta \cos\theta \int_{-\infty}^{+\infty} dE(1+A(E,\theta)-B(E,\theta))(f(E-eV)-f(E)). \tag{2.27}$$

By the same token, the total current flowing across the normal metal - normal metal jucntion is

$$I_{NN}(eV,\theta) = \frac{L^2 e k_F}{4\pi^2\hbar}\int_{-\pi/2}^{+\pi/2} d\theta \cos\theta \int_{-\infty}^{+\infty} dE(1-B(\theta)(f(E-eV)-f(E)), \tag{2.28}$$

where $B(\theta)$ is the reflection probability of the normal metal - normal metal junction. Note that at zero temperature $f(E-eV)$ become a step function, i.e.,

$$f(E-eV)-f(E) = \begin{cases} 1 & E > eV, \\ 0 & E < eV, \end{cases} \tag{2.29}$$

The normalized tunneling current with applied voltage is defined as

$$I(eV,\theta) = \frac{I_{NS}(eV,\theta)}{I_{NN}(eV,\theta)}, \tag{2.30}$$

At zero temperature, the normalized tunneling current is

$$I(eV,\theta) = \frac{\int_{-\pi/2}^{+\pi/2} d\theta \cos\theta \int_{-\infty}^{+\infty} dE(1+A(E,\theta)-B(E,\theta))}{\int_{-\pi/2}^{+\pi/2} d\theta \cos\theta \int_{-\infty}^{+\infty} dE(1-B(\theta))}. \tag{2.31}$$

The tunneling conductance of the normal metal - $d_{x^2-y^2}$-wave superconductor junction is the derivative of the current tunnel across junction with respect to the applied voltage

$$G_{NS}(eV,\theta) = \frac{dI_{NS}(eV,\theta)}{dV}, \tag{2.32}$$

The tunneling conductanc of normal metal - normal metal junction is

$$G_{NN}(eV,\theta) = \frac{dI_{NN}(eV,\theta)}{dV}, \tag{2.33}$$

So, the normalized conductance of the junction is defined as the ratio of the tunneling conductance of normal metal - $d_{x^2-y^2}$-wave superconductor junction to the tunneling conductance of normal metal - normal metal junction:

$$G(eV,\theta) = \frac{G_{NS}(eV,\theta)}{G_{NN}(eV,\theta)}, \tag{2.34}$$

At zero temperature, the normalized tunneling conductance is becomes

$$G(eV,\theta) = \frac{G_{NS}}{G_{NN}} = \frac{\int_{-\pi/2}^{+\pi/2} d\theta \cos\theta (1 + A(E,\theta) - B(E,\theta))}{\int_{-\pi/2}^{+\pi/2} d\theta \cos\theta (1 - B(\theta))}. \tag{2.35}$$

Figure 2.6 shows the plots of the normalized tunneling conductance vs quasiparticle energy E for different value of Z. All the spectra contain peaks at zero energy with different widths and heights. When the strength of barrier increases the width of ZBCP decreases, whereas its height is enhanced.

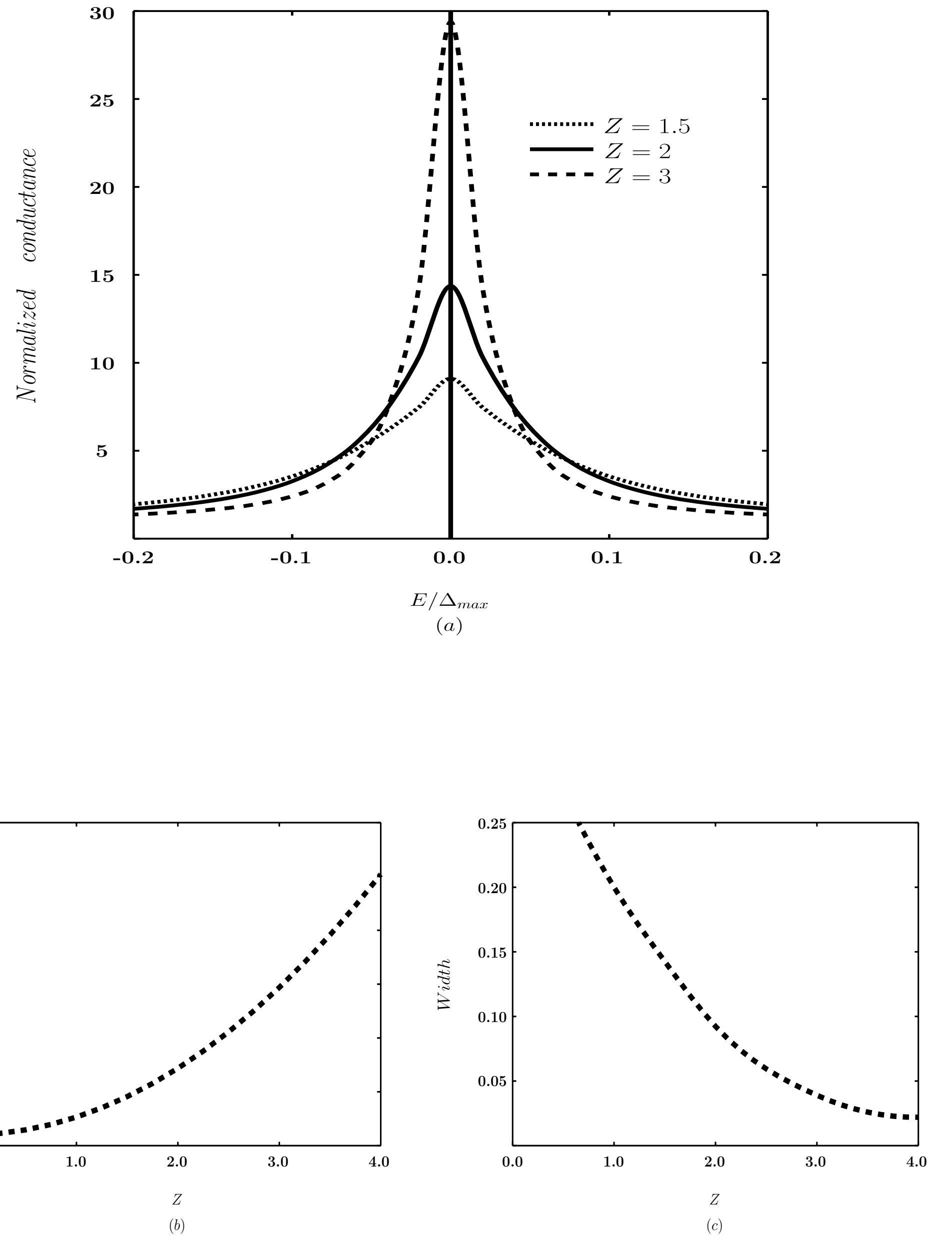

Figure 2.6: (a) The plots of the normalized conductance as a function quasiparticle energy E for different barrier strengths Z= 1.5, 2, 3 at $T = 0$. (b) The plots of the Z dependence of the height of ZBCP. (c) The plots of the Z dependence of the width of ZBCP.

2.3 Conclusions

In this chapter, the ab-plane tunneling spectroscopy of a normal metal - $d_{x^2-y^2}$-wave superconductor junction with $\{110\}$ surface orientation is investigated using the step function model and the BTK formalism. According to this model, the conductance spectrum of $\{110\}$ junction should always contain a ZBCP. This peak is due to the Andreev bound states. Its height and width depend strongly on the transparency of the junction, as show in the plots in Fig. 2.6 (b) and (c). The ZBCP of the junctions with lower transmission has higher height but narrower peak.

Chapter III

The Effect of the Gap Suppression on ZBCP of $\{110\}$ Junctions

3.1 Introduction

The suppression of energy gap of anisotropic superconductors at most surfaces are due to pair breaking. In particular for $d_{x^2-y^2}$-wave superconductors, because the quasiparticles are scattered to branches with different gap values, the pairing can be suppressed and if the different gap values are opposite in sign, zero-energy surface bound states can be formed.

For smooth surfaces, the suppression of $d_{x^2-y^2}$-wave superconducting gap depends on the orientation angle of interface α, which is the angle between the a-axis and the surface normal. Because the $\alpha = 0$ case is analogous to the isotropic s-wave case and corresponds to $\{100\}$ surface, the gap amplitude is not suppressed at surface (see Fig. 3.1).

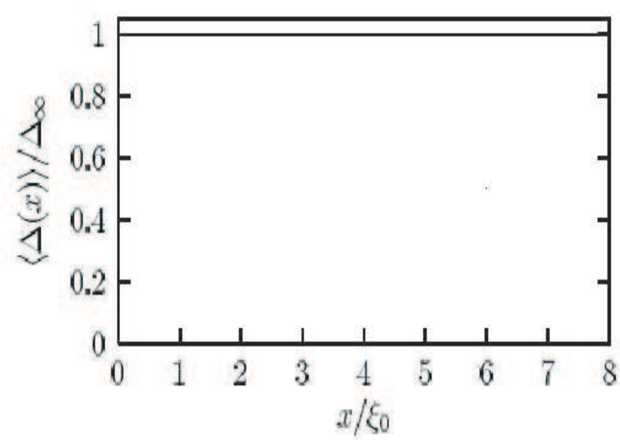

Figure 3.1: The plot of energy gap as a function of x/ξ_0 for a smooth $\alpha = 0$ surface (Lück, T., *et al.*, 2001).

For {110} surfaces ($\alpha = \pi/4$) the gap amplitude is completely suppressed at interface as shown in Fig. 3.2 (Buchholtz, L. J., *et al.*, 1995; Lück, T., *et al.*, 2001).

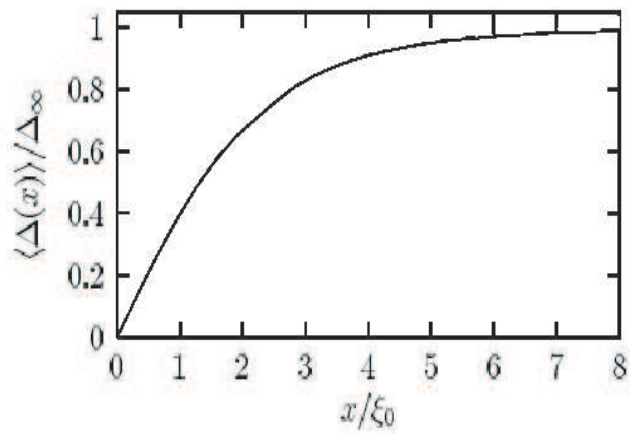

Figure 3.2: The plot of energy gaps as function of x/ξ_0 for a smooth $\alpha = \pi/4$ surface (Lück, T., *et al.*, 2001).

For rough surfaces, the gap function of {100} surface can be suppressed (see Fig. 3.3). The rougher the surface is, the more suppressed the gap can be (Buchholtz, L. J., *et al.*, 1995; Barash, Yu. S., *et al.*, 1997; Lück, T., *et al.*, 2001). For rough {110} surfaces, the gap suppression is no longer complete as shown in Fig. 3.4 (Lück, T., *et al.*, 2001).

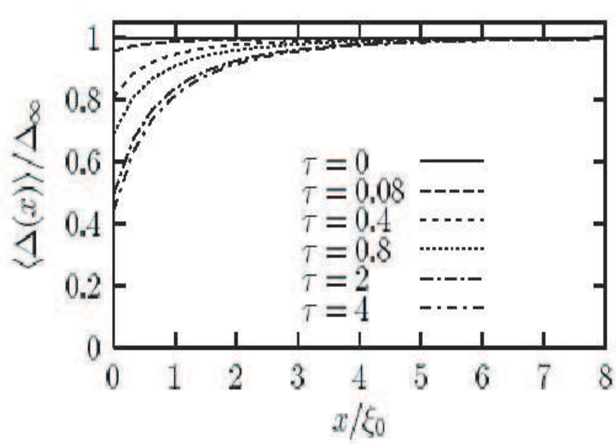

Figure 3.3: The plots of energy gaps for a $\alpha = 0$ surface as a function of x/ξ_0 for several values of surface roughness (τ) (Lück, T., *et al.*, 2001).

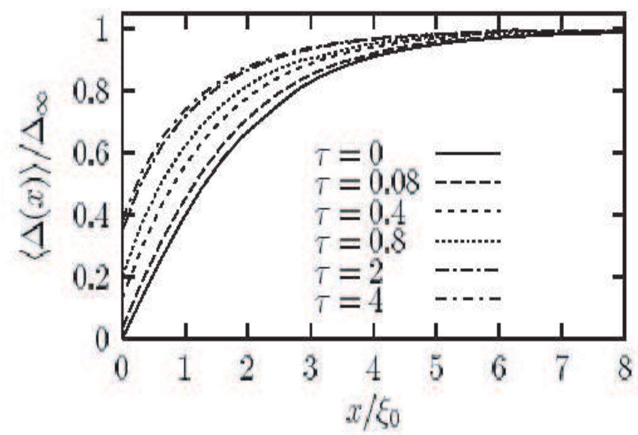

Figure 3.4: The plots of energy gaps for a $\alpha = \pi/4$ surface as a function of x/ξ_0 for several values of the surface roughness (τ) (Lück, T., *et al.*, 2001).

This chapter contains study of the *ab*-plane tunnelling spectroscopy of a normal metal - $d_{x^2-y^2}$-wave superconductor junction with $\{110\}$ surface orientation using a model that includes the suppression of superconducting gap near interface. The effect of the different degrees of suppression on ZBCP is investigated using the BTK formalism. In the next section, the model used to describe the gap near the surface is explained. This section also includes the calculation of all the reflection and transmission coefficients in the framework of the BTK formalism, as well as the calculation of the conductance. Section 3.3 contains the discussion of the effect of the gap suppression on the ZBCP. In section 3.4, the concluding remarks is given.

3.2 The BTK Formalism with the Gap Suppression

The model used to represent a normal metal - $d_{x^2-y^2}$-wave superconductor junction in this chapter is similar to that in the previous chapter. The only difference is that the gap is no longer a step function. It is taken to be dependent on x as

$$\triangle(\vec{k}, x) = \Delta_d(\theta, x) = \triangle_{d0}(\theta, x) + \Big(\Delta_d(\theta, x) - \Delta_{d0}(\theta, x)\Big)\tanh(\frac{x}{\sqrt{2}\xi_l}), \qquad (3.1)$$

where $\Delta_{d0}(\theta, x) = \Delta^0_{max}\sin(2\theta)$ is the $d_{x^2-y^2}$-wave superconducting gap at interface, $\triangle_{d0}(\theta, x) = \triangle_{max}\sin(2\theta)$ is the gap in the bulk, and $\xi_l = \hbar v_F/\Delta_{max}$ is the coherence length.

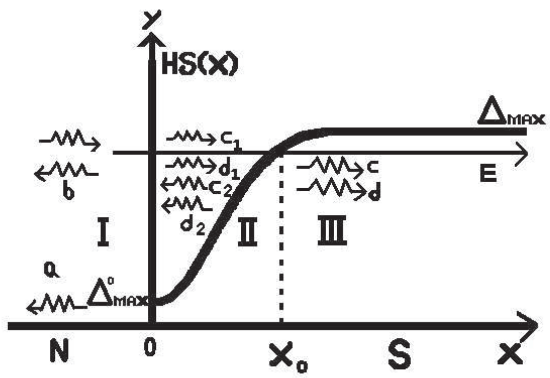

Figure 3.5: The sketch of the normal metal - $d_{x^2-y^2}$-wave superconductor junction with the gap suppression.

In order to obtain the tunnelling conductance spectra of junction, the scattering probabilities are calculated by using the Boliubov-de Gennes equation, where $\triangle(\vec{k}, x)$ is defined in Eq. 3.1. There are 3 regions in this model, as shown in Fig. 3.5.

Region I, $x < 0$, the wave function in this region is

$$\Psi_N(x<0,y) = \left(\begin{bmatrix} 1 \\ 0 \end{bmatrix} e^{iq^+x} + a \begin{bmatrix} 0 \\ 1 \end{bmatrix} e^{-iq^-x} + b \begin{bmatrix} 1 \\ 0 \end{bmatrix} e^{-iq^+x} \right) e^{ik_y y}. \tag{3.2}$$

where a, b are the amplitudes of Andreev and normal reflections, respectively.

Region II, $0 < x < x_0$, where $x_0 = \sqrt{2}E\xi_l/\Delta_{max}$, the wave function is

$$\Psi_{S1}(x>0,y) = \left(c_1 \begin{bmatrix} u_k \\ v_k \end{bmatrix} e^{ik^+x} + d_1 \begin{bmatrix} -v_k \\ u_k \end{bmatrix} e^{-ik^-x} + c_2 \begin{bmatrix} u_k \\ -v_k \end{bmatrix} e^{-ik^+x} + d_2 \begin{bmatrix} v_k \\ u_k \end{bmatrix} e^{ik^-x} \right) e^{ik_y y}. \tag{3.3}$$

where c_1, d_1 are the amplitudes of the two transmitted excitations, and c_2, d_2 are the amplitudes of the two reflected excitations respectively.

Region III, $x > x_0$, the wave function is

$$\Psi_{S2} = \left(c \begin{bmatrix} u_k \\ v_k \end{bmatrix} e^{ik^+x} + d \begin{bmatrix} -v_k \\ u_k \end{bmatrix} e^{-ik^-x} \right) e^{ik_y y}. \tag{3.4}$$

where c, d are the amplitudes of the two transmitted excitations.

The amplitudes a, b, c_1, d_1, c_2, d_2, c, d are obtained by using the matching conditions of the wave functions and of the slopes of the wave function at $x = 0$ and $x = x_0$. These matching conditions are as follows:

$$\begin{aligned} \Psi_N(x=0) &= \Psi_{S1}(x=0) \equiv \Psi(0), \\ \left.\frac{\partial \Psi_{S1}}{\partial x}\right|_{x=0^+} - \left.\frac{\partial \Psi_N}{\partial x}\right|_{x=0^-} &= \frac{2mH}{\hbar^2}\Psi_0, \\ \Psi_{S1}(x=x_0) &= \Psi_{S2}(x=x_0), \\ \left.\frac{\partial \Psi_{S1}}{\partial x}\right|_{x=x_0} &= \left.\frac{\partial \Psi_{S2}}{\partial x}\right|_{x=x_0}. \end{aligned} \tag{3.5}$$

With these boundary conditions, the approximation $\Delta_d(\theta, x) \ll E_F$ and $k_F = q_F$, the reflection and transmission amplitudes can be obtained as follows:

$$\begin{aligned} a(E,\theta) &= \frac{(\frac{2i\cos\theta}{k_F})(u_k v_k' - v_k' u_k) - 4u_k v_k \cos^2\theta}{-(\frac{v_k'^2+u_k'^2}{k_F^2}) - 4v_k^2 Z^2 - 4u_k^2(\cos^2\theta + Z^2) + \frac{4Z}{k_F}(v_k v_k' - u_k u_k')}, \\ b(E,\theta) &= \frac{4iZ(v_k^2 - u_k^2) + \frac{2i\cos\theta + 4Z}{k_F}(v_k v_k' + u_k u_k') - (\frac{v_k'^2+u_k'^2}{k_F^2}) - 4Z^2(u_k^2 + v_k^2)}{(\frac{v_k'^2+u_k'^2}{k_F^2}) + 4v_k^2 Z^2 + 4u_k^2(\cos^2\theta + Z^2) - \frac{4Z}{k_F}(v_k v_k' - u_k u_k')}, \\ c_1(E,\theta) &= \frac{\frac{-2iu_k'\cos\theta}{k_F} - 4u_k\cos\theta(\cos\theta - iZ)}{-(\frac{v_k'^2+u_k'^2}{k_F^2}) - 4v_k^2 Z^2 - 4u_k^2(\cos^2\theta + Z^2) + \frac{4Z}{k_F}(v_k v_k' - u_k u_k')}, \\ d_1(E,\theta) &= \frac{(\frac{2iv_k'\cos\theta}{k_F}) - 4iv_k Z\cos\theta}{(\frac{v_k'^2+u_k'^2}{k_F^2}) + 4v_k^2 Z^2 + 4u_k^2(\cos^2\theta + Z^2) - \frac{4Z}{k_F}(v_k v_k' - u_k u_k')}, \\ c_2(E,\theta) &= 0, \\ d2(E,\theta) &= 0, \\ c(E,\theta) &= \frac{\frac{-2iu_k'\cos\theta}{k_F} - 4u_k\cos\theta(\cos\theta - iZ)}{-(\frac{v_k'^2+u_k'^2}{k_F^2}) - 4v_k^2 Z^2 - 4u_k^2(\cos^2\theta + Z^2) + \frac{4Z}{k_F}(v_k v_k' - u_k u_k')}, \\ d(E,\theta) &= \frac{(\frac{2iv_k'\cos\theta}{k_F}) - 4iv_k Z\cos\theta}{(\frac{v_k'^2+u_k'^2}{k_F^2}) + 4v_k^2 Z^2 + 4u_k^2(\cos^2\theta + Z^2) - \frac{4Z}{k_F}(v_k v_k' - u_k u_k')}, \end{aligned} \tag{3.6}$$

where $u'_k = \frac{\partial u_k}{\partial x}\bigg|_{x=0}$ and $v'_k = \frac{\partial v_k}{\partial x}\bigg|_{x=0}$.

The probabilities $A(E), B(E), C_1(E), D_1(E), C_2(E), D_2(E), C(E), D(E)$ are thus

$$
\begin{aligned}
A(E,\theta) &= |a(E,\theta)|^2|\frac{q^-}{q^+}| = |a(E,\theta)|^2, \\
B(E,\theta) &= |b(E,\theta)|^2|\frac{-q^+}{q^+}| = |b(E,\theta)|^2, \\
C_1(E,\theta) &= |c_1(E,\theta)|^2(|u_k|^2 - |v_k|^2)|\frac{k^+}{q^+}| = |c_1(E,\theta)|^2(|u_k|^2 - |v_k|^2)|, \\
D_1(E,\theta) &= |d_1(E,\theta)|^2(|u_k|^2 - |v_k|^2)|\frac{-k^-}{q^+}| = |d_1(E,\theta)|^2(|u_k|^2 - |v_k|^2)|, \\
C_2(E,\theta) &= 0, \\
D_2(E,\theta) &= 0, \\
C(E,\theta) &= |c(E,\theta)|^2(|u_k|^2 - |v_k|^2)|\frac{k^+}{q^+}| = |c(E,\theta)|^2(|u_k|^2 - |v_k|^2)|, \\
D(E,\theta) &= |d(E,\theta)|^2(|u_k|^2 - |v_k|^2)|\frac{-k^-}{q^+} = |d(E,\theta)|^2(|u_k|^2 - |v_k|^2)|.
\end{aligned} \tag{3.7}
$$

The current and tunnelling conductance of the junction can then be calculated from these probabilities. The conservation of probabilities current density requires

$$
\begin{aligned}
& A(E,\theta) + B(E,\theta) + C_1(E,\theta) + D_{1(}E,\theta) + C_2(E,\theta) \\
& + D_2(E,\theta) + C(E,\theta) + D(E,\theta) = 1,
\end{aligned} \tag{3.8}
$$

In the case where the quasiparticle energy is much less than the maximum gap, $C_1(E,\theta) = D_{1(}E,\theta) = C(E,\theta) = D(E,\theta) = 0$. Thus the relation in Eq. 3.8 becomes

$$
A(E,\theta) + B(E,\theta) = 1. \tag{3.9}
$$

Then the normalized tunnelling conductance of the normal metal - $d_{x^2-y^2}$-wave superconductor junction at zero temperature can be written as

$$
G(eV,\theta) = \frac{G_{NS}}{G_{NN}} = \frac{\int_{-\pi/2}^{+\pi/2} d\theta \cos\theta(1 + A(E,\theta) - B(E,\theta))}{\int_{-\pi/2}^{+\pi/2} d\theta \cos\theta(1 - B(\theta))}. \tag{3.10}
$$

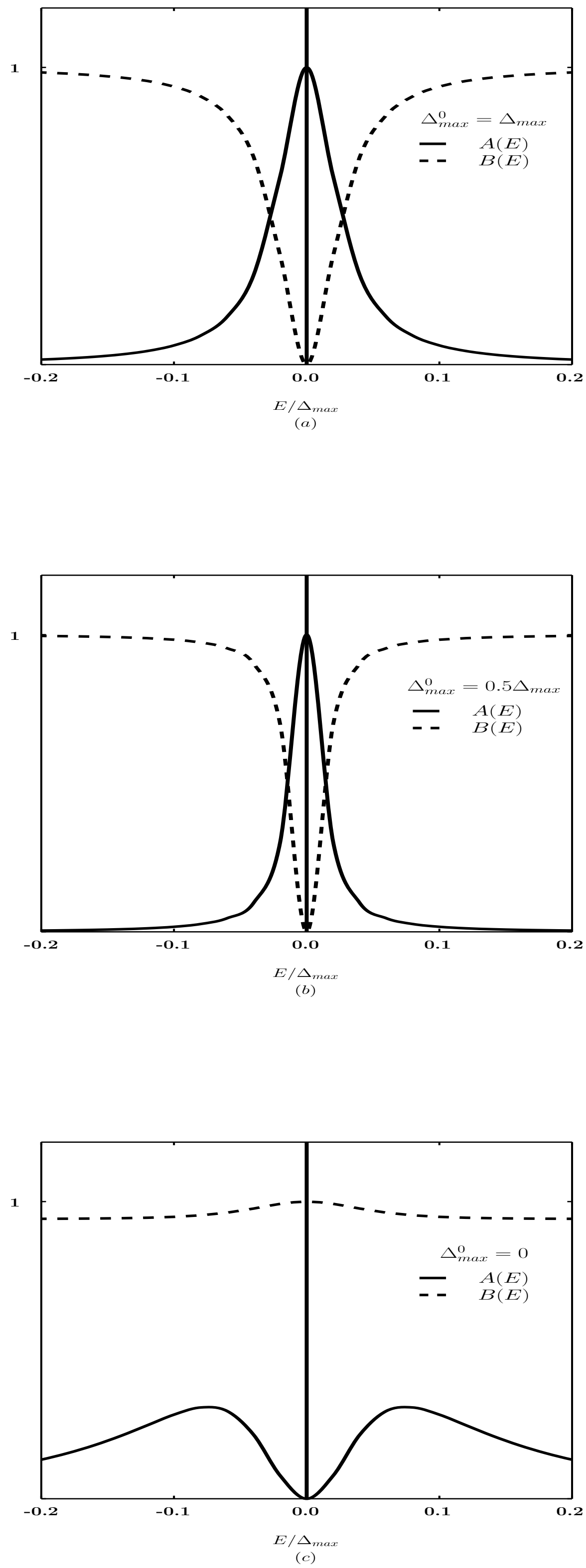

Figure 3.6: The plots of the two reflection coefficients for $Z = 2$ and $\theta = \pi/3$: (a) $\Delta^0_{max} = 1.0\Delta^0_{max}$, (b) $\Delta^0_{max} = 0.5\Delta_{max}$, and (c) $\Delta^0_{max} = 0$.

Fig. 3.6 shows the plots of the Andreev and normal reflection coefficients as a function of energy for $Z = 2$, $\theta = \pi/3$, and different values of the energy gap at the interface, Δ^0_{max}. In the case where $\Delta^0_{max} = \Delta_{max}$ (no gap suppression) and $\Delta^0_{max} = 0.5\Delta_{max}$ (some suppression) as shown in Fig. 3.6 (a) and (b) respectively, it is found that the Andreev reflection peaks at zero energy. The width of the Andreev reflection coefficient depends on the degree of the suppression, i.e., the more the suppression the narrower the peak. As for the case where the suppression is complete, $\Delta^0_{max} = 0$, as shown in Fig. 3.6 (c), the Andreev reflection is zero at zero energy. The absence of the Andreev reflection at zero energy indicates that there is no ZBCP in the tunnelling spectrum in the total suppression case, as will be seen shortly.

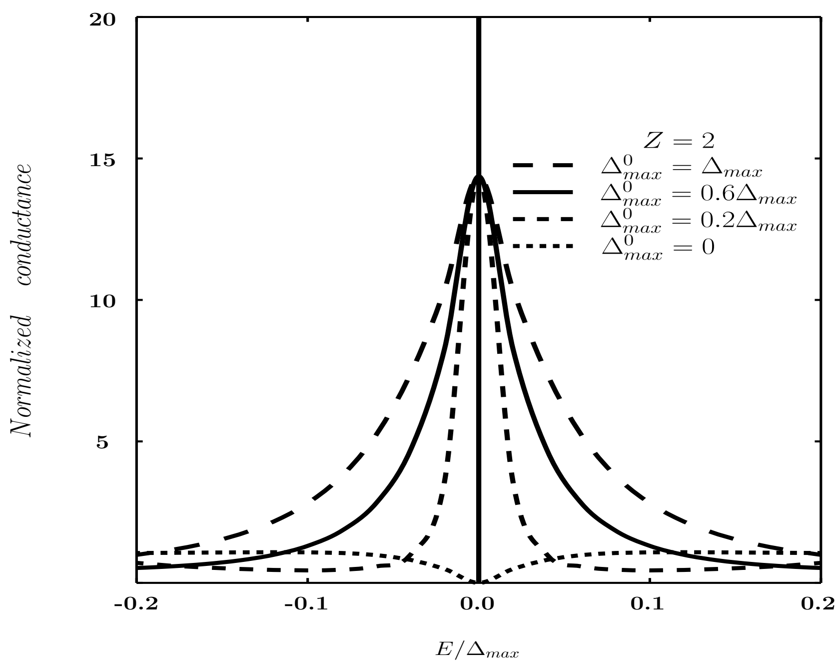

Figure 3.7: The normalized conductance spectra for $Z = 2$ and different values of maximum gap at interface, Δ^0_{max}.

Fig. 3.7 shows the plots of zero-temperature normalized conductance spectra as a function of applied voltage for Z=2 and different values of the energy gap at the interface, Δ^0_{max}. In all cases except one, the ZBCP is present. Different degrees of the gap suppression at the interface lead to different widths of the ZBCP. That is, the smaller Δ^0_{max}, the narrower the ZBCP. The ZBCP does not exist in the case where the gap is totally suppressed at the interface. The reason for the absence ZBCP in this case will be discussed more details in the next section.

3.3 Discussions

As can be seen in the previous section, the characteristics of the ZBCP in the conductance spectrum of {110} junctions depend strongly on the degree of the gap suppression at the interface. ZBCP is absent unless the gap is not completely suppressed. The existence of the ZBCP in {110} junctions of a $d_{x^2-y^2}$-wave superconductor is due to the formation of zero-energy surface bound states (Hu, C-R. 1994; Kashiwaya, S., *et al.*, 1996). These surface bound states are a linear combination of two scattered quasiparticles that have the gap values of opposite sign. The absence of the ZBCP implies that these bound state are not formed and this seems impossible because for {110} junctions the gaps of the two quasiparticles always have opposite signs (see Fig. 3.8). So, the condition for the formation of the zero-energy surface bound states should be looked at more closely.

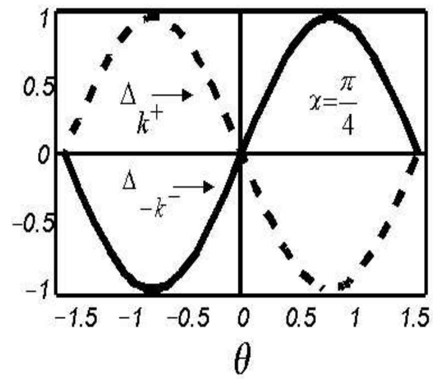

Figure 3.8: The energy gaps of both transmitted excitations for $\alpha = \pi/4$ for every quasiparticle trajectory, $-\pi/2 < \theta < \pi/2$.

Consider a $d_{x^2-y^2}$-wave superconductor-vacuum interface. The wave function of a bound state can be written as a combination of two quasiparticle excitations, as follows:

$$\begin{aligned}
\Psi_S(x>0,y) &= \left(\begin{bmatrix} u_{\kappa^+} \\ v_{\kappa^+} \end{bmatrix} e^{-\kappa^+ x} + R \begin{bmatrix} u_{-\kappa^-} \\ v_{-\kappa^-} \end{bmatrix} e^{-\kappa^- x} \right) e^{i\kappa y}, \\
u_{\kappa^+} &= E - i\sqrt{\Delta^2_{\kappa^+} - E^2}, \\
v_{\kappa^+} &= \Delta_{\kappa^+}, \\
u_{-\kappa^-} &= E + i\sqrt{\Delta^2_{-\kappa^-} - E^2}, \\
v_{-\kappa^-} &= \Delta_{-\kappa^-}, \\
\kappa^{\pm} &= \frac{\sqrt{2m}}{\hbar}\sqrt{E_F \pm \sqrt{\Delta^2_{\kappa^\pm} - E^2}},
\end{aligned} \tag{3.11}$$

where R is reflection amplitude. The surface bound state has the energy less than the smaller of the two gaps: Δ_{κ^+} and $\Delta_{-\kappa^-}$. At the interface, the condition is that $\Psi_s(x=0)=0$. Thus, the energy satisfies one of the following equation,

$$E = \pm|\Delta_{\pm\kappa^\pm}|, \qquad \frac{\Delta_{\kappa^+}(x=0)}{|\Delta_{\kappa^+}(x=0)|} = \frac{\Delta_{-\kappa^-}(x=0)}{|\Delta_{-\kappa^-}(x=0)|}, \tag{3.12}$$

or

$$E = 0, \qquad \frac{\Delta_{\kappa^+}(x=0)}{|\Delta_{\kappa^+}(x=0)|} = \frac{-\Delta_{-\kappa^-}(x=0)}{|\Delta_{-\kappa^-}(x=0)|}. \tag{3.13}$$

The former equation is not acceptable, since it does not lead to a bound state. The latter is the solution for a bound state with zero energy, and the condition for this bound state to exist is that the gaps of the two quasiparticles must have the opposite sign at $x = 0$. When the gaps of the two quasiparticles are zero at $x = 0$, the wave function vanishes and consequently there are no zero-energy bound states.

3.4 Conclusions

In this chapter, the effect of the gap suppression on the tunneling conductance spectra of normal metal - $d_{x^2-y^2}$-wave superconductor $\{110\}$ junctions is investigated using the BTK formalism. It is found that the degree of the gap suppression at the interface strongly affects the characteristics of ZBCP. The more suppressed the gap is, the narrower the ZBCP. If the gap is totally suppressed the conductance spectrum does not contain ZBCP. This finding may be used to explain the absence of ZBCP in many tunneling experiments done in high temperature cuprate superconductors (Cucolo, A. M., *et al.*, 1993; Kane, J., and *et al.*, 1994; Kane, J., and Ng, K.-W. 1996; Wei, J. Y. T., *et al.*, 1998). The degree of the gap suppression depends on many factors, such as the junction orientation (Buchholtz, L. J., *et al.*, 1995; Alber, M., *et al.*, 1996) and surface roughness (Alber, M., *et al.*, 1996; Lück, T., *et al.*, 2001).

Chapter IV

Conclusions

This thesis contains the study of the tunnelling spectroscopy of a normal metal - $d_{x^2-y^2}$-wave superconductor $\{110\}$ junction. In this thesis, the current and the tunneling conductance of the junctions are obtained using the scattering method called the BTK formalism. All the calculations are carried out in the tunneling limit at zero temperature and over the energy rang that is much smaller than the gap maximum of the bulk. The main feature of interest is ZBCP. The results of this study may help explain the absence of ZBCP in some *ab*-plane tunneling spectra of high temperature cuprate superconductors.

In the model without the gap suppression, it is found that the height of ZBCP is proportional to the square of the barrier strength, whereas the width is inversely proportional to the square of the barrier strength. Once the gap suppression is included into the calculations, it is found that, in addition to the dependence on the barrier strength, the height and width of ZBCP depend on the magnitude of the gap at the interface as well. It is also found that ZBCP can be absent if the value of the gap at the interface is zero (total suppression). This finding can be used to explained the absence of ZBCP in many tunneling experiments done on the *ab*-plane tunneling junctions of many high temperature superconductor (Cucolo, A. M., *et al.*, 1994, Wei, J. Y. T., *et al.*, 1998).

The degree of the gap suppression depends on many factors, for example, the interface orientation (Buchholtz, L. J., *et al.*, 1995) and the roughness of the surface (Alber, M., *et al.*, 1996; Lück, T., *et al.*, 2001). In the future work, it is interesting to study the effect of the orientation as well as the roughness on the ZBCP. Other methods of calculations may be needed to do this study. It is also interesting to study the proximity effect on the tunneling spectra of $d_{x^2-y^2}$-wave superconductor, because there are many tunneling experiments done with thin layers of normal metals. These future studies may make the interpretation of the tunneling conductance spectra of high temperature superconductors better.

References

References

Alber, M., Bäuml, B., Ernst, R., Kienle, D., Kopf, A., and Rouchal, M. (1996). Surface boundary conditions for the Ginzburg-Landau theory of d-wave superconductors. **Phys. Rev. B** 53, 5863.

Alff, L., *et al.* (1997). Spatially continuous zero-bias conductance peak on (110) $YBa_2Cu_3O_{7-\delta}$ surface. **Phys. Rev. B** 55, R14757.

Alff, L., *et al.*, (1998). Observation of bound surface states in grain-boundary junctions of high-temperature superconductors. **Phys. Rev. B** 58, 11197.

Andreev, A. F. (1964). The thermal conductivity of the intermediate state in superconductors. **Sov. Phys. JETP.** 19, 1228.

Aubin, H., Greene, L. H., Jian, S., and Hinks, D. G. (2002). Andreev Bound states at the onset of phase coherence in $Bi_2Sr_2CaCuO_8$. **Phys. Rev. Lett.** 89, 177001.

Barash, Yu. S., Svidzinsky, A. A., and Burkhardt, H. (1997). Quasiparticle bound states and low-temperature peaks of the conductance of NIS junctions in d-wave superconductors. **Phys. Rev. B** 55, 15282.

Batlogg, B., *et al.* (1987). Isotope effect in the high-T_c superconductors $Ba_2YCu_3O_7$ and $Ba_2EuCu_3O_7$. **Phys. Rev. Lett.** 58, 2333.

Bednorz, J. G., and Müller, K. A. (1986). High T_c superconductivity in the $BaLaCuO$ system. **Z. Phys. B** 64, 189.

Blonder, G. E., Tinkham, M., and Klapwijk, T. M. (1982). Transition from metallic to tunneling regimes in superconducting microconstrictions: Excess current, charge imbalance, and supercurrent conversion. **Phys. Rev. B** 25, 4515.

Bourne, L. C., Crommie, M. F., Zettl, A., Cohen, M. L., Creager, W. N., and Stacy, A. M. (1987). Onset of superconductivity in $YBaCuO$ at 100 K. **Phys. Rev. Lett.** A120, 494.

Bourne, L. C., *et al*. (1987). Search for isotope effect in superconducting $YBaCuO$. **Phys. Rev. Lett.** 58, 2337.

Brawner, D. A., and Ott, H. R. (1994). Evidence for an unconventional superconducting order parameter in $YBa_2Cu_3O_{6.9}$. **Phys. Rev. B** 50, 6530.

Buchholtz, L. J., Palumbo, M., Rainer, D. and Sauls, J. A. (1995). Thermodynamics of a d-wave superconductor near a surface. **J. Low. Temp. Phys.** 101, 1079.

Burns, G. (1962). **High-temperature superconductivity : An introduction.** New York, Academic Press, Inc.

Wu, C., Xiang, T., and Su, Z-B. (2000). Absence of the zero bias peak in vortex tunneling spectra of high-temperatures superconductors. **Phys. Rev. B** 62, 14427.

Covington, M., *et al*. (1997). Observation of surface-induced broken time-reversal symmetry in $YBa_2Cu_3O_7$ tunnel junction. **Phys. Rev. Lett.** 79, 277.

Cucolo, A. M., Di Leo, R., Nigro, A., Romano, P., and Carotenuto, M. (1994). Different background conductances in the tunneling characteristics of $Bi_2Sr_2CaCuO_8$. **Phys. Rev. B** 49, 1308.

Duke, C. B. (1969). **Tunneling in solids**. New York, Academic Press, Inc.

Fogelström, M., Rainer, D., and Sauls, J. A. (1997). Tunneling into current-carrying surface states of high-T_c superconductor. **Phys. Rev. B** 79, 281.

Giaever, I. (1960). Energy gap in superconductors measured by electron tunneling. **Phys. Rev. Lett.** 5, 147.

Hu, C-R. (1994). Midgap surface states as a novel signature for $d_{x_a^2-x_b^2}$ -wave superconductivity. **Phys. Rev. Lett.** 72, 1526.

Iguchi, I., Wang, W., Kashiwaya, S., Tanaka, Y., Koyamagi, M., and Kajimura, K. (1996). Theory for tunneling spectroscopy of anisotropic superconductors. **Phys. Rev. B** 53, 2667.

Iguchi, I., Wang, W., Yamazaki, M., Tanaka, Y., and Kashiwaya, S. (2000). Angle-resolved andreev bound states in anisotropic d-wave high-T_c $YBa_2Cu_3O_{7-y}$ superconductors. **Phys. Rev. B** 62, R6131.

Kane, J., Chen Q., Ng, K.-W., and Tao H.-J. (1994). Observation of ab-plane gap anisotropy in $Bi_2Sr_2CaCu_2O_8$ with a low temperature scanning tunneling microscope. **Phys. Rev. Lett.** 72, 128.

Kane, J., and Ng, K.-W. (1996). Angular dependence of the in-plane energy gap of $Bi_2Sr_2CaCu_2O_8$ by tunneling spectroscopy. **Phys. Rev. B** 53, 2819.

Kashiwaya, S., Tanaka, Y., Koyanaki, M., Takashima, H., and Kajimura, K. (1995). Origin of zero-bias conductance peaks in high-T_c superconductors. **Phys. Rev. B** 51, 1350.

Kashiwaya, S., Tanaka, Y. Koyanaki, M., and Kajimura, K. (1996). Theorey for tunneling spectroscopy of anisotropic superconductor. **Phys. Rev. B** 53, 2667.

Kirtley, J. R., *et al.* (1996). Direct imaging of integer and half-integer josephson vortices in high-T_c grain boundaries. **Phys. Rev. Lett.** 76, 1336.

Lück, T., Eckern, U., and Shelankov, A. (2001). d-wave superconductors near surfaces and interface: A scattering matrix approach within the quasiclassical technique. **Phys. Rev. B** 63, 064510.

Maeda, H., Tanaka, Y., Fukutomi, N., and Asano, T. (1988). Superconducting properties of $CuS2 - xSex$. **Jpn. J. Appl. Phys.** 27, L209.

Mascarenhas, A., Katayama-Yoshida, H., Pankove, J., and Deb, S. K. (1989). Copper isotope effect in Raman scattering on superconducting $YBa_2Cu_3O_{7-x}$. **Phys. Rev. B** 39, 4699.

Mortensen, N. A. (1998). **Theoretical models of transport in macroscopic and mesoscopic NS structures.** Master's Thesis, Technical University of Denmark.

Pairor, P., and Walker, M. B. (2002). Tunneling conductance for d-wave superconductors: Dependence on crystallographic orientation and Fermi surface. **Phys. Rev. B** 65, 064507.

Parks, R. D. (1996). **Superconductivity** (Vols. 1). New York, Marcel dekker, Inc.

Pascal, J. Y., Schwarz, R. B., Pierce, C. B., Bernardez, L., Conners, A., and Meisenhelimer, R. (1989). Oxygen isotope effect in $YBa_2Cu_3O_7$ prepared by burning YBa_2Cu_3 in O^{16} and O^{18}. **Phys. Rev. B** 39, 6690.

Sinha, S., and Ng, K.-W. (1998). Zero bias conductance peak enhancement in $Bi_2Sr_2CaCu_2O_8/Pb$ tunneling junctions. **Phys. Rev. Lett.** 80, 1296.

Tanaka, Y., and Kashiwaya, S. (1995). Theory of tunneling spectroscopy of d-wave superconductors. **Phys. Rev. Lett.** 74, 3451.

Tanaka, Y., and Kashiwaya, S. (1996). Local density of states of quasiparticles near the interface of nonuniform d-wave superconductors. **Phys. Rev. B** 53, 9371.

Tinkham, M. (1996). **Introduction to superconductivity**. 2nd ed, New York, McGraw-Hill, Inc.

Tsuei, C. C., *et al*. (1994). Pairing symmetry and flux quantization in a tricrystal superconducting ring of $YBa_2Cu_3O_{7-\delta}$. **Phys. Rev. Lett.** 73, 593.

Wei, J. Y. T., Tsuei, C. C., van Bentum, P. J. M., Xiong, Q., Chu, C. W., and Wu, M. K. (1998). Quasiparticle tunneling specrta of the high T_c mercury cuprates: Implications of the d-wave two-dimensional van Hove scenario. **Phys. Rev. B** 57, 3650.

Wolf, E. L. (1985). **Principles of electron tunneling spectroscopy**. NewYork, Oxford university Press.

Wollman, D. A., van Harlingen, D. J., Lee, W. C., Ginsberg, D. M., and Leggtt, A. J. (1993). Experimental determination of the superconducting pairing state in $YBCO$ from the phase coherence of $YBCO$-Pb dc SQUIDs. **Phys. Rev. Lett.** 71, 2134.

Wu, M. K., *et al*. (1987). Superconductivity at 93 K in a new mixed-phase $YBaCuO$ compound system at ambient pressure. **Phys. Rev. Lett.** 58, 908.

Curriculum Vitae

NAME: Sukanya Nilmoung

GENDER: Female

NATIONALITY: Thai

DATE OF BIRTH: June 9, 1978

MARITAL STATUS : Single

EDUCATION BACKGROUND:

- High School 1997.
- B.Sc. 2001 (Applied-Physics), Mahasarakham University, Thailand.